

# ON THE RELATIONSHIP BETWEEN RADIO EMISSION AND BLACK HOLE MASS IN GALACTIC NUCLEI

LUIS C. HO

The Observatories of the Carnegie Institution of Washington,  
 813 Santa Barbara St., Pasadena, CA 91101  
*To appear in The Astrophysical Journal.*

## ABSTRACT

We use a comprehensive database of black hole masses ( $M_{\text{BH}}$ ) and nuclear luminosities to investigate the relationship between radio emission and  $M_{\text{BH}}$ . Our sample covers a wide range of nuclear activity, from nearby inactive nuclei to classical Seyfert 1 nuclei and luminous quasars. Contrary to some previous studies, we find that the radio continuum power, either integrated for the entire galaxy or isolated for the core, correlates poorly with  $M_{\text{BH}}$ . The degree of nuclear radio loudness, parameterized by the radio-to-optical luminosity ratio  $R$ , also shows no clear dependence on  $M_{\text{BH}}$ . Radio-loud nuclei exist in galaxies with a wide range of  $M_{\text{BH}}$ , from  $10^6 M_\odot$  to a few  $10^9 M_\odot$ , and in a variety of hosts, from disk-dominated spirals to giant ellipticals. We demonstrate that  $R$  is strongly inversely correlated with  $L=L_E$ , the ratio of nuclear luminosity to the Eddington luminosity, and hence with mass accretion rate. Most or all of the weakly active nuclei in nearby galaxies are radio-loud, highly sub-Eddington systems that are plausibly experiencing advection-dominated accretion.

*Subject headings:* black hole physics — galaxies: active — galaxies: nuclei — galaxies: quasars — galaxies: Seyfert — radio continuum: galaxies

## 1. INTRODUCTION

Efforts to search for massive black holes (BHs) in the centers of nearby galaxies have made rapid progress in the last few years (Kormendy & Richstone 1995; Richstone et al. 1998; van der Marel 1999; Ho 1999a; Kormendy & Gebhardt 2001). Kinematic observations of a significant number of galaxies have yielded evidence for central dark objects with masses  $10^6 - 10^9 M_\odot$ , which can be plausibly interpreted as massive BHs. In two cases, namely the center of the Milky Way and NGC 4258, the extraordinarily high density of the dark matter appears to rule out all reasonable astrophysical alternatives to a single collapsed object (Maoz 1998). To date, BH masses are available for 40 inactive or weakly active galaxies from observations of spatially resolved kinematics and for a comparable number of bright active galactic nuclei (AGNs) from “reverberation mapping” of their broad-line regions (see § 2.1 and Table 1), sufficient to encourage preliminary examinations of statistical relationships between BH masses and global properties of the galaxies. Two correlations have emerged for the weakly active galaxies: (1)  $M_{\text{BH}}$  correlates with  $L_{\text{bulge}}$ , the optical luminosity (/ mass) of the bulge component of the galaxy (Kormendy 1993; Kormendy & Richstone 1995; Magorrian et al. 1998; Ho 1999a; Kormendy & Gebhardt 2001), and (2)  $M_{\text{BH}}$  correlates even more strongly with  $\sigma_e$ , the luminosity-weighted stellar velocity dispersion within the bulge effective radius  $r_e$  (Gebhardt et al. 2000b; Ferrarese & Merritt 2000). By contrast,  $M_{\text{BH}}$  depends little on disk properties (Kormendy et al. 2001). These empirical relations hold great promise for furthering our understanding of the formation of massive BHs, the formation of galaxy spheroids, and the apparent close connection between the two.

Another correlation which has received considerable attention is that between  $M_{\text{BH}}$  and radio emission. Franceschini, Vercellone, & Fabian (1998) compiled a sample of the dozen BH masses known as of mid-1997 and showed that they evidently scale with radio luminosity, approximately of the form  $L_{\text{rad}} / M_{\text{BH}}^{2.5}$ , where  $L_{\text{rad}}$  is measured at 5 GHz (6 cm). Sur-

prisingly, the correlation is as tight, if not tighter, for the total radio emission integrated over galactic scales than it is for the core emission alone. They (see also Di Matteo, Carilli, & Fabian 2001) argue that the functional form of the  $L_{\text{rad}} - M_{\text{BH}}$  relation arises naturally if the BH accretion takes the form of an advection-dominated accretion flow (ADAF; see Narayan, Mahadevan, & Quataert 1998b and Quataert 2001 for reviews), fueled by hot gas from a large-scale spherical inflow. Moreover, the steepness of the relation gives it considerable leverage in predicting  $M_{\text{BH}}$  efficiently from  $L_{\text{rad}}$ , a readily available quantity. Several subsequent studies similarly considered related samples of nearby galaxies, but their results have been mixed (Yi & Bough 1999; Salucci et al. 1999; Laor 2000; Di Matteo et al. 2001). Discussion of the apparent dependence of  $M_{\text{BH}}$  on radio luminosity and the radio-loudness parameter ( $R$ ) recently has also surfaced in the context of more active galaxies such as Seyferts and quasars (McLure et al. 1999; Nelson 2000; Laor 2000; McLure & Dunlop 2001; Lacy et al. 2001; Gu, Cao, & Jiang 2001).

This paper reexamines the relationship between radio emission and  $M_{\text{BH}}$  in light of the most up-to-date samples of active and weakly active galaxies with reliable BH mass measurements. We show that the loose trend between integrated radio luminosity and  $M_{\text{BH}}$  is largely indirect, a consequence of more fundamental correlations between radio luminosity and bulge mass on the one hand, and between bulge mass and  $M_{\text{BH}}$  on the other. The distribution of nuclear radio luminosity as a function of  $M_{\text{BH}}$  is more physically grounded, but its large scatter renders it ineffective as a statistical tool to predict  $M_{\text{BH}}$ . The  $R - M_{\text{BH}}$  relation disappears altogether when one considers AGNs with a broad range of intrinsic luminosities. However, we find that  $R$  is strongly related to the mass accretion rate.

## 2. THE DATABASE

We begin with a fairly detailed documentation of the data used in the subsequent analysis. Particular attention is paid to the source of the  $M_{\text{BH}}$  measurements (Table 1) and photometric parameters (Table 2).

TABLE 1: GALAXIES WITH BLACK HOLE MASSES

Galaxy Name (1)	Hubble Type (2)	$T$ (3)	Spectral Class (4)	$cz$ (km s <sup>-1</sup> ) (5)	$D$ (Mpc) (6)	Ref. (7)	$M_{\text{BH}}$ ( $M_{\odot}$ ) (8)	Method (9)	Ref. (10)
3C 120 (Mrk 1506)	S0:	-1.0	S1	9896	137.8	1	$2.3 \times 10^7$	R	1
3C 390.3 (VII w 838)	E?	-5.0	S1	16818	241.2	1	$3.4 \times 10^8$	R	1
Ark 120 (Mrk 1095)	S0/a	0.0	S1	9682	134.6	1	$1.84 \times 10^8$	R	1
Arp 102B	E0	-5.0	L1.8	7245	99.7	1	$2.2 \times 10^8$	G	2
Circinus	Sb:	3.0	S2	449	4.0	2	$1.3 \times 10^6$	M	3
Fairall 9	S?	...	S1	14095	199.8	1	$8.0 \times 10^7$	R	1
IC 342	SABcd	6.0	H	31	1.8	3	$< 5.0 \times 10^5$	S	4
IC 1459	E3	-5.0	L2	1691	29.2	4	$3.7 \times 10^8$	G	5
IC 4329A	S0+	-1.0	S1	4813	65.5	1	$5.0 \times 10^6$	R	1
Milky Way	Sbc	3.0	...	...	0.008	5	$2.95 \times 10^6$	S	6
Mrk 79 (UGC 3973)	SBb	3.0	S1.5	6652	91.3	1	$5.2 \times 10^7$	R	1
Mrk 110	Pair?	...	S1	10580	147.7	1	$5.6 \times 10^6$	R	1
Mrk 279 (UGC 8823)	S0	-1.0	S1.5	9129	126.6	1	$4.2 \times 10^7$	R	1
Mrk 335	S0/a	0.0	S1.0	7730	106.6	1	$6.3 \times 10^6$	R	7
Mrk 509	comp	...	S1	10312	143.8	1	$5.78 \times 10^7$	R	1
Mrk 590 (NGC 863)	Sa:	1.0	S1.2	7910	109.2	1	$1.78 \times 10^7$	R	1
Mrk 817 (UGC 9412)	S?	...	S1.5	9430	131.0	1	$4.4 \times 10^7$	R	1
NGC 205 (M110)	dE5	-5.0	A	-241	0.74	6	$< 9.3 \times 10^4$	S	8
NGC 221 (M32)	E2	-6.0	A	-145	0.81	4	$3.9 \times 10^6$	S	9
NGC 224 (M31)	Sb	3.0	A	-300	0.76	4	$3.3 \times 10^7$	S	10
NGC 598 (M33)	Scd	6.0	H	-179	0.87	6	$< 1.5 \times 10^3$	S	11
NGC 821	E6?	-5.0	A	1735	24.1	4	$5.0 \times 10^7$	S	12
NGC 1023	SB0-	-3.0	A	637	11.4	4	$3.9 \times 10^7$	S	13
NGC 1068 (M77)	Sb	3.0	S1.9	1137	14.4	7	$1.6 \times 10^7$	M	14
NGC 2778	E	-5.0	...	2049	22.9	4	$2.0 \times 10^7$	S	12
NGC 2787	SB0+	-1.0	L1.9	696	7.5	4	$3.9 \times 10^7$	G	15
NGC 3031 (M81)	Sab	2.0	S1.5	-34	3.9	4	$6.3 \times 10^7$	S	16
NGC 3115	S0-	-3.0	A	720	9.7	4	$9.1 \times 10^8$	S	17
NGC 3227	SABa	1.0	S1.5	1157	20.6	7	$3.9 \times 10^7$	R	1
NGC 3245	S0?	-2.0	T2	1358	20.9	4	$2.1 \times 10^8$	G	18
NGC 3377	E5+	-5.0	A	665	11.2	4	$1.0 \times 10^8$	S	12
NGC 3379 (M105)	E1	-5.0	L2/T2:	911	10.6	4	$1.0 \times 10^8$	S	19
NGC 3384	SB0-:	-3.0	A	704	11.6	4	$1.8 \times 10^7$	S	12
NGC 3516	SB0:	-2.0	S1.2	2649	38.9	7	$2.3 \times 10^7$	R	7
NGC 3608	E2	-5.0	L2/S2:	1253	22.9	4	$1.1 \times 10^8$	S	12
NGC 3783	SBa	1.0	S1	2917	38.5	7	$9.4 \times 10^6$	R	1
NGC 3998	S0?	-2.0	L1.9	1040	14.1	4	$5.6 \times 10^8$	S	16
NGC 4051	SABbc	4.0	S1.2	725	17.0	7	$1.3 \times 10^6$	R	1
NGC 4151	SABab	2.0	S1.5	995	20.3	7	$1.53 \times 10^7$	R	1
NGC 4203	SAB0	-3.0	L1.9	1086	14.1	4	$< 1.2 \times 10^7$	G	15
NGC 4258 (M106)	SABbc	4.0	S1.9	448	7.3	4	$4.1 \times 10^7$	M	20
NGC 4261 (3C 270)	E2+	-5.0	L2	2238	31.6	4	$5.2 \times 10^8$	G	21
NGC 4291	E	-5.0	A	1757	26.2	4	$1.5 \times 10^8$	S	12
NGC 4342	S0-	-3.0	...	751	16.8	7	$3.4 \times 10^8$	S	22
NGC 4374 (M84, 3C 272.1)	E1	-5.0	L2	1060	18.4	4	$1.6 \times 10^9$	G	23
NGC 4395	Sm:	9.0	S1.5	319	3.6	7	$< 1.1 \times 10^5$	S	24
NGC 4459	S0+	-1.0	T2:	1210	16.1	4	$6.5 \times 10^7$	G	15
NGC 4473	E5	-5.0	A	2244	15.7	4	$1.0 \times 10^8$	S	12
NGC 4486 (M87, 3C 274)	E0+	-4.0	L2	1307	16.1	4	$3.4 \times 10^9$	G	25

TABLE 1: GALAXIES WITH BLACK HOLE MASSES—*Continued*

Galaxy Name (1)	Hubble Type (2)	$T$ (3)	Spectral Class (4)	$cz$ (km s <sup>-1</sup> ) (5)	$D$ (Mpc) (6)	Ref. (7)	$M_{\text{BH}}$ ( $M_{\odot}$ ) (8)	Method (9)	Ref. (10)
NGC 4486B	E0	-6.0	...	1555	16.1	8	$6.0 \times 10^8$	S	26
NGC 4564	E	-5.0	A	1142	15.0	4	$5.7 \times 10^7$	S	12
NGC 4593	SBb	3.0	S1	2698	39.5	7	$8.1 \times 10^6$	R	7
NGC 4594 (M104)	Sa	1.0	L2	1024	9.8	4	$1.1 \times 10^9$	S	27
NGC 4596	SB0	-1.0	L2::	1874	16.8	7	$5.8 \times 10^7$	G	15
NGC 4649 (M60)	E2	-5.0	A	1117	16.8	4	$2.0 \times 10^9$	S	12
NGC 4697	E6	-5.0	...	1241	11.7	4	$1.2 \times 10^8$	S	12
NGC 4945	SBcd	6.0	S2	560	4.2	9	$1.1 \times 10^6$	M	28
NGC 5548	S0/a	0.0	S1.5	5149	70.2	1	$1.23 \times 10^8$	R	1
NGC 5845	E	-5.0	...	1456	25.9	4	$3.2 \times 10^8$	S	12
NGC 6251	E0	-5.0	S2	6900	94.8	1	$5.4 \times 10^8$	G	29
NGC 7052	E4	-5.0	...	4672	63.6	1	$3.6 \times 10^8$	G	30
NGC 7457	S0-?	-3.0	A	812	13.2	4	$3.4 \times 10^6$	S	12
NGC 7469	SABa	1.0	S1.0	4892	66.6	1	$6.5 \times 10^6$	R	1
PG 0026+129	...	...	QSO	0.142	627.4	1	$5.4 \times 10^7$	R	1
PG 0052+251	S	...	QSO	0.155	690.4	1	$2.2 \times 10^8$	R	1
PG 0804+761	...	...	QSO	0.100	429.9	1	$1.89 \times 10^8$	R	1
PG 0844+349	...	...	QSO	0.064	268.4	1	$2.16 \times 10^7$	R	1
PG 0953+414	S	...	QSO	0.239	1118	1	$1.84 \times 10^8$	R	1
PG 1211+143	...	...	QSO	0.085	361.7	1	$4.05 \times 10^7$	R	1
PG 1226+023 (3C 273)	E	...	QSO	0.158	705.1	1	$5.5 \times 10^8$	R	1
PG 1229+204	S	...	QSO	0.064	268.4	1	$7.5 \times 10^7$	R	1
PG 1307+085	E	...	QSO	0.155	690.4	1	$2.8 \times 10^8$	R	1
PG 1351+640	...	...	QSO	0.087	370.7	1	$4.6 \times 10^7$	R	1
PG 1411+442	...	...	QSO	0.089	379.8	1	$8.0 \times 10^7$	R	1
PG 1426+015 (Mrk 1383)	...	...	QSO	0.086	366.2	1	$4.7 \times 10^8$	R	1
PG 1613+658 (Mrk 876)	...	...	QSO	0.129	565.3	1	$2.41 \times 10^8$	R	1
PG 1617+175 (Mrk 877)	...	...	QSO	0.114	494.7	1	$2.73 \times 10^8$	R	1
PG 1700+518	...	...	QSO	0.292	1406	1	$6 \times 10^7$	R	1
PG 1704+608 (3C 351)	E	...	QSO	0.371	1857	1	$3.7 \times 10^7$	R	1
PG 2130+099	...	...	QSO	0.061	255.3	1	$1.44 \times 10^8$	R	1

NOTE.— Col. (1) Galaxy name. Col. (2) Revised Hubble type from de Vaucouleurs et al. 1991 (RC3), except for QSOs, which is estimated by Hamilton, Casertano, & Turnshek 2001. Col. (3) Morphological type index from the RC3. Col. (4) Spectral class of the nucleus from Ho et al. 1997, and otherwise from Whittle 1992a and NED, where A = absorption-line nucleus, H = H II nucleus, L = LINER, S = Seyfert, T = “transition object” (LINER/H II), 1 = type 1, 2 = type 2, and a fractional number between 1 and 2 denotes various intermediate types; uncertain and highly uncertain classifications are followed by a single and double colon, respectively. Col. (5) Heliocentric radial velocity (redshift for QSOs) from NED. Col. (6) Adopted distance. Col. (7) Reference for  $D$ . Col. (8) Black hole mass, scaled to our adopted distances. Col. (9) Method for determining  $M_{\text{BH}}$ : G, gas kinematics; M, maser kinematics; R, reverberation mapping; S, stellar kinematics. Col. (10) Reference for  $M_{\text{BH}}$ .

REFERENCES.— *Distance*: (1) Luminosity distance derived from heliocentric redshift,  $H_0 = 75 \text{ km s}^{-1} \text{ Mpc}^{-1}$ ,  $\Omega_{\text{M}} = 0.3$ , and  $\Omega_{\Lambda} = 0.7$ ; (2) Freeman et al. 1977; (3) McCall 1989; (4) Tonry et al. 2001; (5) Reid 1993; (6) Ferrarese et al. 2000; (7) Tully 1988, who also uses our value of  $H_0$ ; (8) Assumed to be at the distance of NGC 4486; (9) Assumed to be at the distance of NGC 5128, which is known from Tonry et al. 2001.

REFERENCES.— *Black hole mass*: (1) Kaspi et al. 2000; (2) Newman et al. 1997; (3) Greenhill et al. 2000; (4) Böker, van der Marel, & Vacca 1999; (5) Verdoes Kleijn et al. 2000; (6) Genzel et al. 2000; (7) Ho 1999a; (8) Jones et al. 1996; (9) van der Marel et al. 1998; (10) Kormendy & Bender 1999; (11) Gebhardt et al. 2001; (12) Gebhardt et al. 2000a; (13) Bower et al. 2001a; (14) Greenhill et al. 1996; (15) Sarzi et al. 2001; (16) Bower et al. 2001b; (17) Emsellem, Dejonghe, & Bacon 1999; (18) Barth et al. 2001; (19) Gebhardt et al. 2000b; (20) Miyoshi et al. 1995; (21) Ferrarese, Ford, & Jaffe 1996; (22) Cretton & van den Bosch 1999; (23) Bower et al. 1998; (24) Filippenko & Ho 2001; (25) Macchetto et al. 1997; (26) Kormendy et al. 1997a; (27) Kormendy et al. 1997b; (28) Greenhill, Moran, & Herrnstein 1997; (29) Ferrarese & Ford 1999; (30) van der Marel & van den Bosch 1998.

TABLE 2: PHOTOMETRIC PARAMETERS

Galaxy Name	$A_B$ (mag)	$M_{B_T}^0$ (mag)	$\log P_{6,\text{tot}}$ (W Hz $^{-1}$ )	Ref.	$\log P_{6,\text{nuc}}$ (W Hz $^{-1}$ )	Ref.	$\log L_{H\beta}$ (erg s $^{-1}$ )	Ref.	$M'_B$ (mag)	$\log R'$
(1)	(2)	(3)	(4)	(5)	(6)	(7)	(8)	(9)	(10)	(11)
3C 120	1.28	-21.93	24.90	1	24.90	1	42.13	1	-20.79	2.85
3C 390.3	0.31	-21.42	25.62	2	25.62	2	42.24	2	-21.12	3.44
Ark 120	0.55	-22.10	22.43	3	21.80	3	42.75	3	-22.62	-0.98
Arp 102B	0.10	-19.61	23.28	1	22.87	4	41.05	4	-17.59	2.11
Circinus	6.22	-22.13	21.10	4	21.04	5	41.59	5	-19.19	-0.37
Fairall 9	0.12	-23.12	<22.96	5	<22.96	1	42.92	3	-23.13	<-0.03
IC 342	2.41	-19.59	20.03	1	17.95	5	36.46	6	-4.01	2.61
IC 1459	0.068	-21.43	23.07	6	23.02	6	39.14	7	-11.94	4.51
IC 4329A	0.26	-20.34	22.26	3	22.25	7	41.61	3	-19.25	0.82
Milky Way	...	-20.53	21.04	7	15.79	8	32.73	8	7.03	4.86
Mrk 79	0.31	-21.21	22.07	3	21.62	9	41.84	3	-19.93	-0.09
Mrk 110	0.056	-19.84	22.15	3	21.76	9	41.66	3	-19.40	0.26
Mrk 279	0.068	-20.47	22.15	8	22.09	10	41.83	3	-19.90	0.40
Mrk 335	0.15	-21.65	21.60	8	21.60	10	42.16	3	-20.88	-0.48
Mrk 509	0.25	-21.14	22.40	3	22.11	11	42.70	3	-22.48	-0.61
Mrk 590	0.16	-21.31	22.04	8	21.91	10	40.99	3	-17.42	1.21
Mrk 817	0.029	-21.18	22.03	8	22.05	10	41.93	3	-20.20	0.24
NGC 205	0.27	-15.70	<16.67	3	<17.12	12	<34.40	6	<2.09	...
NGC 221	0.27	-15.78	<16.75	3	<16.89	12	<35.82	6	<-2.12	...
NGC 224	0.27	-20.31	18.40	1	15.40	13	38.60	9	-10.34	-2.47
NGC 598	0.18	-18.61	17.25	3	<16.70	14	34.61	6	1.47	<3.55
NGC 821	0.47	-20.71	<19.70	3	<19.54	15	<37.78	6	<-7.92	...
NGC 1023	0.26	-20.19	<19.05	3	...	...	<37.42	6	<-6.85	...
NGC 1068	0.15	-21.33	22.73	1	22.43	16	40.67	3	-16.47	2.11
NGC 2778	0.090	-18.54	<19.65	3	<19.58	15	...	10	...	...
NGC 2787	0.57	-18.13	19.61	3	19.78	12	37.90	6	-8.27	2.74
NGC 3031	0.35	-20.42	20.39	1	20.23	17	38.69	11	-10.61	2.25
NGC 3115	0.21	-20.27	<18.91	3	<18.57	18	<37.67	6	<-7.59	...
NGC 3227	0.098	-20.57	21.25	8	21.20	17	40.14	3	-14.90	1.51
NGC 3245	0.11	-20.01	20.30	3	20.24	15	38.89	6	-11.20	2.02
NGC 3377	0.15	-19.16	<19.03	3	<18.88	15	...	10	...	...
NGC 3379	0.11	-20.00	19.29	3	19.03	18	37.72	6	-7.74	2.20
NGC 3384	0.12	-19.59	<19.06	3	<18.91	15	<37.40	6	<-6.79	...
NGC 3516	0.18	-20.63	21.28	8	21.34	17	41.18	3	-17.98	0.42
NGC 3608	0.090	-20.19	20.54	3	<19.50	15	37.81	6	-8.00	<2.56
NGC 3783	0.51	-21.09	21.63	3	21.36	16	41.53	3	-19.01	0.02
NGC 3998	0.069	-19.21	21.29	1	21.29	19	39.48	12	-12.95	2.37
NGC 4051	0.056	-20.38	20.60	8	20.54	17	39.96	3	-14.37	1.06
NGC 4151	0.12	-20.16	21.79	8	21.84	17	41.37	3	-18.54	0.68
NGC 4203	0.052	-19.00	19.92	3	20.43	17	38.68	6	-10.58	2.46
NGC 4258	0.069	-20.29	21.29	1	19.35	17	37.84	6	-8.09	2.38
NGC 4261	0.078	-21.17	23.69	1	22.58	19	38.58	6	-10.28	4.73
NGC 4291	0.16	-19.82	<19.77	3	<19.43	18	<37.82	6	<-8.03	...
NGC 4342	0.088	-17.81	<19.39	3	<19.23	15	...	10	...	...
NGC 4374	0.17	-21.40	23.16	3	22.15	20	38.31	6	-9.48	4.62
NGC 4395	0.074	-17.21	19.15	9	18.29	17	37.63	12	-7.47	1.57
NGC 4459	0.20	-19.91	<19.35	3	19.39	15	38.23	6	-9.25	1.96
NGC 4473	0.12	-19.94	<19.33	3	<19.77	15	<37.53	6	<-7.18	...
NGC 4486	0.096	-21.54	24.27	1	23.09	21	38.78	6	-10.88	5.01
NGC 4486B	0.092	-16.76	<19.35	3	...	...	...	10	...	...
NGC 4564	0.15	-18.98	<19.29	3	<19.13	15	<37.27	6	<-6.41	...
NGC 4593	0.11	-20.26	20.68	3	20.48	16	41.12	3	-17.80	-0.38
NGC 4594	0.22	-21.20	21.25	10	21.15	22	38.59	6	-10.31	3.29
NGC 4596	0.096	-19.88	<19.39	3	<19.23	15	37.65	6	-7.53	<2.48
NGC 4649	0.11	-21.43	20.73	3	20.78	23	<37.27	6	<-6.41	>4.49
NGC 4697	0.13	-20.33	<19.07	3	<19.01	24	...	10	...	...
NGC 4945	0.76	-19.58	21.81	6	21.59	25	39.97	13	-14.40	2.09

TABLE 2: PHOTOMETRIC PARAMETERS—*Continued*

Galaxy Name	$A_B$ (mag)	$M_{B_T}^0$ (mag)	$\log P_{6,\text{tot}}$ (W Hz $^{-1}$ )	Ref.	$\log P_{6,\text{nuc}}$ (W Hz $^{-1}$ )	Ref.	$\log L_{H\beta}$ (erg s $^{-1}$ )	Ref.	$M'_B$ (mag)	$\log R'$
(1)	(2)	(3)	(4)	(5)	(6)	(7)	(8)	(9)	(10)	(11)
NGC 5548	0.088	−21.02	21.91	8	21.86	17	41.72	3	−19.58	0.29
NGC 5845	0.23	−18.80	<19.76	3	<19.60	15	...	10	...	...
NGC 6251	0.38	−21.40	24.18	2	24.22	26	38.79	14	−10.90	6.13
NGC 7052	0.52	−20.73	22.77	1	22.64	27	39.22	15	−12.18	4.03
NGC 7457	0.22	−18.73	<19.18	3	...		<36.82	6	<−5.07	...
NGC 7469	0.29	−21.41	22.58	8	22.47	17	41.81	3	−19.84	0.79
PG 0026+129	0.31	−24.35	23.38	11	23.38	1	43.42	16	−24.61	−0.19
PG 0052+251	0.21	−23.99	22.63	11	22.63	1	43.40	16	−24.55	−0.93
PG 0804+761	0.15	−23.17	22.72	11	22.72	1	43.21	16	−23.99	−0.61
PG 0844+349	0.16	−23.30	21.43	11	21.43	1	43.07	16	−23.57	−1.74
PG 0953+414	0.054	−25.24	23.45	11	23.45	1	44.17	16	−26.83	−1.01
PG 1211+143	0.15	−23.31	24.39	11	24.39	1	43.11	16	−23.69	1.18
PG 1226+023	0.089	−26.47	27.34	11	27.34	1	44.51	16	−27.83	2.48
PG 1229+204	0.12	−22.61	21.76	11	21.76	1	42.95	16	−23.22	−1.26
PG 1307+085	0.15	−24.07	22.30	11	22.30	1	43.61	16	−25.17	−1.51
PG 1351+640	0.088	−22.52	23.34	11	23.34	1	42.65	16	−22.33	0.67
PG 1411+442	0.036	−22.95	22.02	11	22.02	1	43.08	16	−23.60	−1.15
PG 1426+015	0.14	−22.91	22.29	11	22.29	1	42.98	16	−23.31	−0.77
PG 1613+658	0.11	−23.43	23.06	11	23.06	1	43.29	16	−24.22	−0.36
PG 1617+175	0.18	−23.06	22.50	11	22.50	1	43.16	16	−23.84	−0.76
PG 1700+518	0.15	−25.46	24.23	11	24.23	1	43.79	16	−25.70	0.22
PG 1704+608	0.097	−25.50	26.71	11	26.71	1	43.52	16	−24.90	3.01
PG 2130+099	0.19	−22.61	22.20	11	22.20	1	42.95	16	−23.22	−0.82

NOTE.— Col. (1) Galaxy name. Col. (2) Galactic extinction in the  $B$  band, based on the DIRBE/*IRAS* maps of Schlegel, Finkbeiner, & Davis 1998 and the extinction law of Cardelli, Clayton, & Mathis 1989. Col. (3) Total absolute  $B$  magnitude, corrected for Galactic extinction; data for nearby galaxies from RC3 or LEDA; data for PG QSOs from Schmidt & Green 1983; data for Milky Way assuming  $M_K = -24.06$  mag (Malhotra et al. 1996) and  $B - K = 3.53$  mag (for  $T = 3$ ; de Jong 1996). Col. (4) Logarithm of the total 6 cm spectral power obtained from low-resolution (beam  $\gtrsim 1'$  in most cases) observations; in a few cases where 6 cm data are unavailable we extrapolated measurements from other wavelengths assuming  $f_\nu \propto \nu^{-0.5}$ , as found by Ho & Ulvestad 2001. Col. (5) Reference for  $P_{6,\text{tot}}$ . Col. (6) Logarithm of the nuclear 6 cm spectral power. Col. (7) Reference for  $P_{6,\text{nuc}}$ . Col. (8) Logarithm of the  $H\beta$  (narrow + broad components) luminosity, corrected for Galactic extinction. Col. (9) Reference for  $L_{H\beta}$ . Col. (10) Absolute  $B$  magnitude of the nucleus, obtained from the  $L_{H\beta} - M_B$  relation of Ho & Peng 2001. Col. (11) Logarithm of the ratio of the nuclear luminosities in the radio to the optical  $B$  band, defined as  $R' \equiv L_\nu(6 \text{ cm})/L'_\nu(B)$ , with  $L'_\nu(B)$  computed from  $M'_B$ .

REFERENCES.— *Integrated radio emission*: (1) Becker, White, & Edwards 1991, resolution 3.5; (2) White & Becker 1992, resolution 12', extrapolated from 20 cm; (3) Condon et al. 1998, resolution 0.75, extrapolated from 20 cm; (4) Gregory et al. 1994, resolution 4.2; (5) Whittle 1992a, extrapolated from 20 cm; (6) Wright et al. 1996, resolution 4.2; (7) Berkhuysen 1984, extrapolated from 408 MHz assuming  $f_\nu \propto \nu^{-0.7}$ ; (8) Rush, Malkan, & Edelson 1996, resolution 1.5; (9) Condon 1987, resolution 1', extrapolated from 20 cm; (10) Griffith et al. 1994, resolution 4.2; (11) Kellermann et al. 1989.

REFERENCES.— *Nuclear radio emission*: (1) Assumed to be equal to the total radio power; (2) Barvainis, Lonsdale, & Antonucci 1996; (3) Puschell et al. 1986; (4) Elmouttie et al. 1998; (5) Turner & Ho 1983; (6) Sadler, Jenkins, & Kotanyi 1989; (7) Unger et al. 1987, extrapolated from 20 cm; (8) Ekers et al. 1983, for Sgr A\* only; (9) Ulvestad & Wilson 1984a; (10) Kukula et al. 1995, extrapolated from 3.6 cm; (11) Singh & Westergaard 1992; (12) Heckman, Balick, & Crane 1980; (13) Crane, Dickel, & Cowan 1992, extrapolated from 3.6 cm; (14) Hummel et al. 1987, extrapolated from 20 cm; (15) Wrobel & Heeschen 1991; (16) Ulvestad & Wilson 1984b; (17) Ho & Ulvestad 2001; (18) Fabbiano, Gioia, & Trinchieri 1989; (19) Wrobel & Heeschen 1984; (20) Jenkins, Pooley, & Riley 1977; (21) Biretta, Stern, & Harris 1991; (22) Hummel, van der Hulst, & Dickey 1984; (23) Spencer & Junor 1986; (24) Birkinshaw & Davies 1985; (25) Elmouttie et al. 1997; (26) Jones et al. 1986; (27) Morganti et al. 1987.

REFERENCES.— *Nuclear H $\beta$  emission*: (1) Tadhunter et al. 1993; (2) Oke & Goodrich 1981; (3) Whittle 1992a; (4) Halpern et al. 1996; (5) Oliva et al. 1994, corrected for extinction; (6) Ho, Filippenko, & Sargent 1997; (7) Verdoes Kleijn et al. 2000; (8) extrapolated from the  $L_X(2 - 10 \text{ keV}) - L_{H\alpha}$  relation of Ho et al. 2001, based on the *Chandra* 2 – 10 keV detection of Sgr A\* reported by Baganoff et al. 2001; (9) Heckman 1996, spatially integrated over the central few hundred pcs; (10) no  $H\beta$  measurement available; optical continuum upper limit (given in col. 11) obtained from archival *HST* image, following the method of Ho & Peng 2001 and Ravindranath et al. 2001; (11) Ho, Filippenko, & Sargent 1996; (12) unpublished, but based on data from Ho et al. 1995, 1997; (13) Moorwood & Oliva 1988, based on Br $\gamma$  flux and an intrinsic ratio  $H\beta/\text{Br}\gamma = 36$  appropriate for Case B recombination in low-density gas at  $T_e = 10^4$  K (Osterbrock 1989); (14) Shuder & Osterbrock 1981; (15) Morganti, Ulrich, & Tadhunter 1992 give the flux of  $H\alpha + [\text{N II}]$ , which we use, along with the  $[\text{N II}]/H\alpha$  ratio of van den Bosch & van der Marel 1995, to estimate the  $H\beta$  flux; (16) Boroson & Green 1992, obtained from  $H\beta$  equivalent widths and optical continuum flux densities (see Ho & Peng 2001).

### 2.1. Black Hole Masses

Our primary sample of BH masses comes from spatially resolved observations of gas and stellar kinematics. Reviews of these methods can be found in Kormendy & Richstone (1995) and Ho (1999a). Table 1 represents an update of the compilation of BH masses given in Ho (1999a), supplemented with newly published values. The majority of the gas measurements consist of optical observations of ionized gaseous disks, all done with the *Hubble Space Telescope* (*HST*); four galaxies (Circinus, NGC 1068, NGC 4258, and NGC 4945) exploit the availability of strong water maser emission to probe the nuclear kinematics using radio interferometry. The broad-line radio galaxy Arp 102B presents a special case in which a periodic signature in its emission-line light curve has been interpreted as the orbital period of an accretion disk (Newman et al. 1997). With the exception of Sgr A in the Galactic Center, whose mass has been determined through proper motions and radial velocities of individual stars (Eckart & Genzel 1997; Ghez et al. 1998; Genzel et al. 2000), all the stellar-based masses come from integrated spectroscopy, a few from the ground, but largely from *HST*.

Magorrian et al. (1998) published  $M_{\text{BH}}$  for a significant number of nearby early-type galaxies based on axisymmetric, two-integral dynamical modeling of *HST* images and ground-based stellar spectroscopy. We do not use these masses, however, because they are subject to considerable uncertainties due to the simplified modeling and the low spatial resolution of the spectra. As commented by a number of authors (van der Marel 1999; Ferrarese & Merritt 2000; Gebhardt et al. 2000b), the two-integral assumption will tend to overestimate  $M_{\text{BH}}$ . We illustrate this explicitly for the 16 galaxies in Magorrian et al.’s sample that overlap with the sample assembled in Table 1 (Fig. 1). The average offset for these objects is a factor of 3.3. Figure 1b indicates that the discrepancy seems to be slightly more severe for “core” galaxies than for “power-law” galaxies, systems with and without a resolved break in their inner surface brightness profiles, respectively (Lauer et al. 1995; Faber et al. 1997). As a class, core galaxies tend to be luminous, pressure-supported systems with boxy isophotes (e.g., Faber et al. 1997; Ravindranath et al. 2001), precisely those most prone to having an anisotropic velocity distribution and thus most ill-suited for two-integral modeling. Figure 1b offers mild support for this picture.

We include several meaningful upper limits. Four come from stellar-kinematical constraints placed on the central nuclear star cluster (IC 342, M33, NGC 205, and NGC 4395), and a fifth derives from *HST* gas kinematics (NGC 4203).

Direct dynamical measurements become unfeasible for luminous or distant AGNs. The bright continuum emission of the active nucleus nearly always overpowers the stellar absorption lines near the center, and in many cases the extended line emission can be strongly perturbed by nongravitational forces. For these objects we must rely on more indirect methods to estimate the central masses. A promising technique employs “reverberation mapping” (Blandford & McKee 1982) to determine the size of the broad-line region,  $r$ , which when combined with a characteristic velocity dispersion of the line-emitting gas,  $\sigma$ , as reflected in the observed line widths, yields an estimate of the virial mass,  $M_{\text{vir}} = r^2 \sigma^2 / G$ . Choosing  $\sigma = \frac{\sqrt{3}}{2} \text{FWHM(H)} / 2$  for random, isotropic orbits, several studies have computed virial masses in this fashion for Seyfert 1 nuclei (Ho 1999a; Wandel, Peterson, & Malkan 1999) and low-redshift quasars (Kaspi et

al. 2000). Ho (1999a) used  $\text{FWHM(H)} / 2$  from single-epoch spectra, whereas Wandel et al. (1999) argue that the variable component (rms) of the spectrum should yield a more faithful representation of the velocity field associated with the time lag used to calculate  $r$ . As Wandel et al. note, however, the simple expectation that time-averaged spectra should yield narrower line widths than rms spectra appear not to hold in all objects. In practice, it seems difficult to justify one choice over the other (Kaspi et al. 2000). A more serious uncertainty lies in the choice of  $\sigma$ . McLure & Dunlop (2001) advocate that a disk component with  $\sigma = \frac{\sqrt{3}}{2} \text{FWHM(H)} / 2$  yields  $M_{\text{BH}}$  values for AGNs that agree better with the  $M_{\text{BH}}-L_{\text{bulge}}$  relation for weakly active galaxies, thereby obviating the apparent discrepancy found by Ho (1999a) and Wandel (1999). The situation is far from clear, however, since AGN masses computed assuming random orbits agree, to first order, with the  $M_{\text{BH}}-L_{\text{e}}$  relation (Gebhardt et al. 2000c; Nelson 2000; Ferrarese et al. 2001). Notwithstanding this and other possible systematic uncertainties (Krolik 2001), reverberation mapping appears capable of delivering  $M_{\text{BH}}$  for AGNs with an accuracy of a factor of 2–3.

Table 1 lists  $M_{\text{BH}}$  based on reverberation mapping for 20 Seyfert 1 galaxies and 17 low-redshift quasars. For the sake of uniformity, we use the compilation of Kaspi et al. (2000) for the majority of the objects; a few not included in that study were taken from Ho (1999a).

Galaxy distances enter linearly into the mass determination for all methods except reverberation mapping, wherein the size scale depends only on the light-travel time between the central continuum source and the line-emitting gas. Thus, it is important to pay close attention to the reliability of the adopted distances. Whenever possible we use Tonry et al.’s (2001) homogeneous database of distances based on *I*-band surface brightness fluctuations.

### 2.2. Nuclear Luminosities

Our subsequent analysis primarily will examine the connection between  $M_{\text{BH}}$  and two measures of the radio output, namely the absolute spectral power and the radio-to-optical luminosity ratio. Since we are interested in quantities pertaining to the nucleus, we take great effort to assemble *nuclear* radio and optical data. As emphasized in several recent studies of low-luminosity galactic nuclei (Ho 1999c; Ho et al. 2000, 2001; Ho & Peng 2001), high angular resolution is of paramount importance for isolating the central emission from the surrounding galaxy.

For the radio band, we make use of interferometric data obtained at 6 cm with beam sizes  $< 5''$ . The nuclear 6 cm spectral power,  $P_{6\text{cm}}$ , computed from the observed flux densities assuming isotropic emission, represents the integrated emission from all components considered associated with the “active” (nonstellar) nucleus. In the case of the brighter AGNs, this often includes some extended structures, such as jet-like linear features, in addition to the central core. For comparison with recent results from the literature, we have also collected radio data for the integrated emission from the whole galaxy (host plus nucleus),  $P_{6\text{cm, tot}}$ , which we approximate with low-resolution (beam  $> 1''$ ) measurements. A minority of the data were acquired at wavelengths other than 6 cm, and these were extrapolated to 6 cm assuming  $f \propto \nu^{-0.5}$ , the median spectrum between 6 and 20 cm for Seyfert nuclei found by Ho & Ulvestad (2001).

Ho & Peng (2001) demonstrated the utility of *HST* images

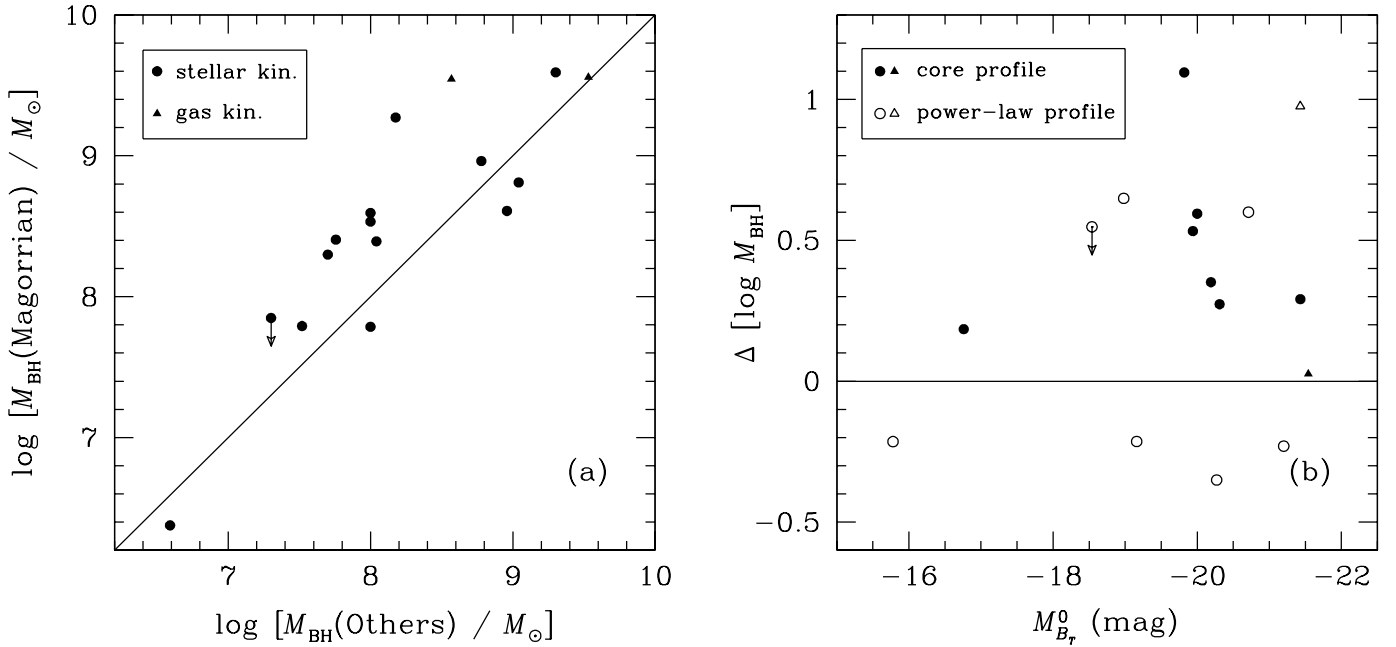


FIG. 1.— (a) Comparison between black hole masses from Magorrian et al. (1998) with those obtained from others. The masses from Magorrian et al. are systematically higher. (b) The difference in  $\log M_{\text{BH}}$  as a function of the luminosity and surface brightness profile of the galaxy. The solid line denotes equality. The most discrepant masses are found in luminous galaxies with core-type profiles.

for separating the optical continuum cores in a sample of nearby Seyfert 1 galaxies. Although *HST* images are available for most of the weakly active galaxies, here we take a different approach. A number of the objects have type 2 nuclei<sup>1</sup>, which, according to the AGN unification picture (Antonucci 1993), implies that the nuclear continuum should be hidden from direct view, or at least appreciably extinguished. Instead, we estimate the continuum strength indirectly through the known (Yee 1980; Shuder 1981) correlation between H $\alpha$  luminosity and *B*-band absolute magnitude for type 1 AGNs, as recently calibrated by Ho & Peng (2001). The line luminosity (broad and narrow components combined) is, in principle, a more isotropic quantity than the optical continuum luminosity. We collected nuclear Balmer-line luminosities (or upper limits thereof for sources lacking line emission), translated them to H $\alpha$  if necessary<sup>2</sup> (only for a few cases; see Table 2), and then applied the  $L_{\text{H}\alpha}$ – $M_B$  conversion (Ho & Peng 2001) to arrive at  $M_B^0$ . We use the notation  $M_B^0$  to distinguish it from the directly measured quantity  $M_B$ . Note that  $M_B$  is available for all the quasars (Schmidt & Green 1983) and for a number of the Seyfert 1 nuclei (Ho & Peng 2001); for the bright, variable Seyfert nuclei studied with reverberation mapping, it can be ascertained quite reliably from the published spectrophotometry. For internal consistency, however, we follow the same procedure as adopted for the weakly active sample.

As discussed in Ho & Peng (2001), the individual line luminosities can be quite uncertain, and the low-luminosity end of the  $L_{\text{H}\alpha}$ – $M_B$  relation has significant scatter. We do not expect the continuum magnitudes to be very accurate for any given object, but it is hoped that the statistical results are more robust.

We use the spectral radio luminosity and the optical nuclear luminosity to calculate the equivalent of the standard radio-

loudness parameter  $R$ ,  $R^0 = L(6\text{ cm})/L^0(B)$ . Following common practice (Visnovsky et al. 1992; Stocke et al. 1992; Kellermann et al. 1994), we set the boundary between “radio-loud” and “radio-quiet” classes at  $R^0 = 10$ .

### 2.3. The Special Case of the Galactic Center

The Galactic Center warrants some individual attention. Because of its proximity, the “nucleus” of the Milky Way — identified with Sgr A — is overresolved with respect to other galaxies, thus rendering comparisons somewhat ambiguous. In our subsequent discussions, we relax the definition of the Galactic Center to include increasingly larger areas surrounding Sgr A. At radio wavelengths, two distinct regions can be identified in the vicinity of Sgr A, namely Sgr A West and Sgr A East (Ekers et al. 1983). Each of the latter two components is  $\sim 40$  times brighter than Sgr A at 6 cm. To achieve a linear scale roughly equivalent to that sampled in most of the external galaxies, however, one must extend to dimensions of  $1'' \times 1''$ , or approximately 150 pc  $\times$  150 pc. The 6 cm flux density on this scale (600 Jy; Mezger & Pauls 1979) is roughly 10 times higher than the entire Sgr A complex combined.

Evaluating the radio-loudness parameter for the Galactic Center requires knowledge of its intrinsic optical continuum luminosity, ideally measured on the various scales discussed above for the radio emission. The optical emission, of course, is not directly observable because of the tremendous opacity along our line of sight. Instead, we proceed as follows. We utilize the luminosity measured in the hard X-ray (2–10 keV) band, corrected for photoelectric absorption, to estimate the intrinsic (unextinguished) H $\alpha$  luminosity using the relation between  $L_{\text{X}}(2-10\text{ keV})$  and  $L_{\text{H}\alpha}$  proposed by Ho et al. (2001) for nearby galactic nuclei. Next,  $L_{\text{H}\alpha}$  follows straightforwardly from  $L_{\text{H}}$

<sup>1</sup> Type 1 and type 2 AGNs are defined as those with and without detectable broad emission lines, respectively.

<sup>2</sup> We adopt an intrinsic ratio of H $\alpha$ /H $\beta$  = 3.1, as might be appropriate for the physical conditions in active nuclei (e.g., Gaskell & Ferland 1984).

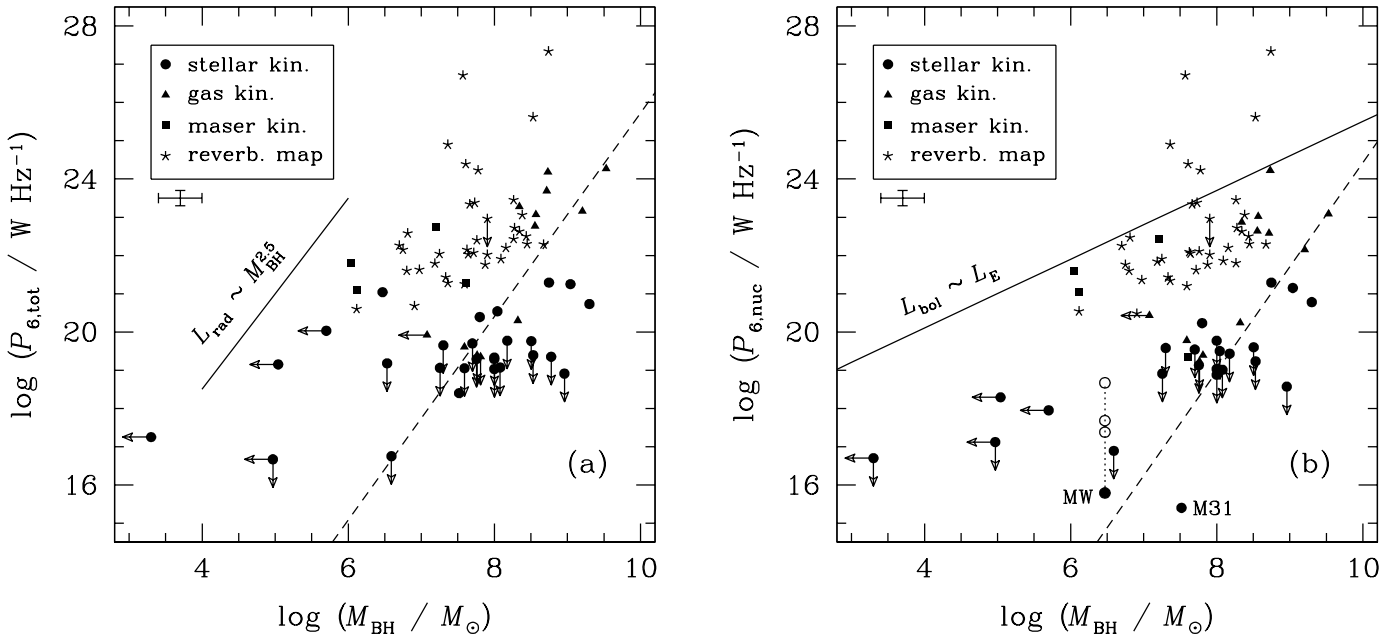


FIG. 2.— Dependence of (a) total and (b) nuclear 6 cm spectral power on black hole mass. The symbols for the different methods of mass determination are given in the legend, below which representative error bars are plotted. Arrows indicate upper limits. The *dashed line* in each graph gives the regression fit proposed by Franceschini et al. (1998); the *solid lines* are discussed in the text. In panel (b) we have labeled the outlier M31. Four values of  $P_{6,\text{nuc}}$  are given for the Milky Way (MW), connected by the *dotted line*; in increasing value, they are for Sgr A, Sgr A West, Sgr A West+East, and the central 1'' (150 pc 150 pc) (see § 2.3).

for an assumed  $H/\text{H}$  ratio. And finally, the relation between  $L_H$  and  $M_B$  (Ho & Peng 2001) yields the  $B$ -band continuum flux density needed to calculate the  $R$  parameter.

Baganoff et al. (2001) recently detected Sgr A unambiguously in the hard X-rays with *Chandra*; the unabsorbed 2–10 keV luminosity has a surprisingly low value of  $2.4 \times 10^{33} \text{ erg s}^{-1}$ . The hard X-ray emission on larger scales comes from observations performed using *ASCA* by Koyama et al. (1996). On dimensions which encompass Sgr A West,  $L_X(2-10 \text{ keV}) = 7.7 \times 10^{35} \text{ erg s}^{-1}$ , while for the 1'' 1'' region they find  $L_X(2-10 \text{ keV}) = 7.7 \times 10^{36} \text{ erg s}^{-1}$ . We could not locate a definitive value for the X-ray luminosity of Sgr A East. Following the above procedure, we find that Sgr A, Sgr A West, and the 1'' 1'' region have  $\log R = 4.9, 3.8$ , and  $4.0$ , respectively. The Galactic Center, irrespective of one's exact definition of its boundaries, evidently is extremely “radio loud” according to the conventional  $R$  parameterization.

Admittedly, the above conclusions for the Galactic Center depend strongly on the applicability of the conversion factors used to translate  $L_X(2-10 \text{ keV})$  to  $M_B$ , ones which were originally derived for more luminous, more active type 1 nuclei (see Ho et al. 2001; Ho & Peng 2001). The spectral classification of the Galactic Center is unknown. Ho et al. (2001) find that type 2 nuclei with detectable X-ray cores generally have  $L_X/L_H$  values that are a factor of 10 lower than in type 1 objects. Even a factor of 10 error, or greater, however, cannot erase the large  $R$  values given above. And although a direct relation between  $L_H$  and  $M_B$  does not exist for type 2 objects (the optical continuum is weak or obscured), to the extent that the line emission is powered by photoionization and  $M_B$  traces the low-energy tail of the ionizing continuum, the two quantities should roughly scale with one another in type 2 objects as they do in type 1 systems.

#### 2.4. Error Estimates

Systematic errors affect many of the quantities used in this paper. Although formal uncertainties are not specified explicitly for the data presented in Tables 1 and 2, we wish to alert the reader of their likely magnitude and impact on our analysis. The representative error bars shown in the figures of this paper are meant to capture the assessment given in this section.

Ho & Peng (2001; see § 3.3) give a fairly thorough account of the error budget associated with the radio and optical luminosities. We will not repeat the details here, except to reiterate that the typical uncertainties for the radio powers, optical line luminosities, and  $R^0$  are 0.2, 0.3, and 0.5 dex, respectively.

At the moment, the uncertainties on  $M_{\text{BH}}$  are still quite varied. The masses for the BHs in the Galactic Center (Genzel et al. 2000) and NGC 4258 (Miyoshi et al. 1995) are known with high confidence, on the order of 10%. Masses based on three-integral modeling of stellar kinematics are accurate to

0.3 dex on average (Gebhardt et al. 2000b), but the few that are still based on two-integral models may undergo more significant revisions in the future. While it is generally thought that gas-kinematical methods are less prone to modeling uncertainties than those based on stellar kinematics, under some circumstances our inability to treat realistically certain effects such as asymmetric drift may lead to serious systematic errors. In the case of IC 1459, the effect of asymmetric drift on  $M_{\text{BH}}$  may be as large as a factor of 4 (Verdoes Kleijn et al. 2000). This correction, on the other hand, is much less significant in NGC 3245, whose  $M_{\text{BH}}$  has been determined to an accuracy of 25% (Barth et al. 2001). Lastly, we concluded in § 3.1 that reverberation-mapping masses are probably accurate to a factor of 2–3. Thus, an overall uncertainty of 0.3 dex for  $M_{\text{BH}}$  seems



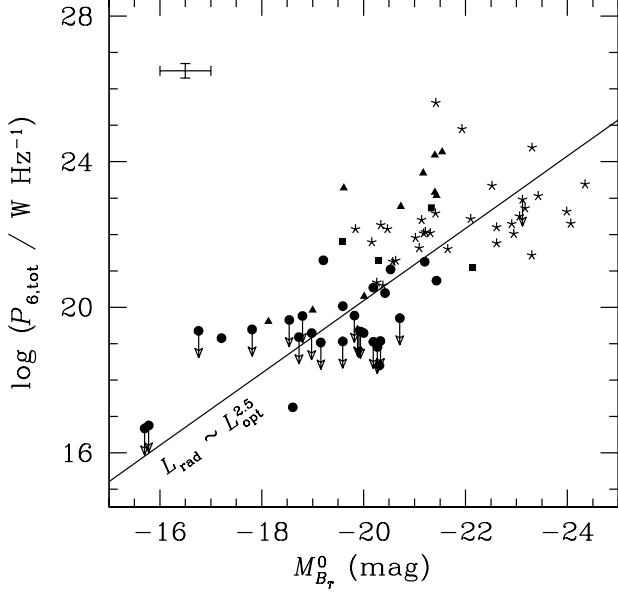


FIG. 3.— Dependence of total 6 cm spectral power on the absolute  $B$  magnitude of the galaxy. Symbols as in Figure 2. Representative error bars are plotted in the upper left corner; arrows indicate upper limits. The solid line shows the formal linear regression fit.

reasonable.

### 3. PARAMETER CORRELATIONS

#### 3.1. Radio Power and Black Hole Mass

Concentrating first on the purported dependence of total radio power on  $M_{\text{BH}}$ , Figure 2a shows that these two quantities are *not* well correlated for the sample of weakly active galaxies, contrary to the results of Franceschini et al. (1998). Laor (2000) recently arrived at a similar conclusion using the less reliable (see § 2.1) BH masses from Magorrian et al. (1998). Although the best-fit regression line proposed by Franceschini et al. ( $L_{\text{rad}} / M_{\text{BH}}^{2.5}$ ; dashed line) does roughly follow the trend of the data, the scatter about the fit is enormous. The distribution of points may be tracing an upper envelope. The absence of points on the upper left corner of the diagram is real: luminous radio sources associated with low-mass BHs (which preferentially inhabit low-mass bulges) can hardly be missed. The lower right portion of the graph, on the other hand, is mostly populated by upper limits, and the remaining blank region may reflect the observational bias against finding faint radio sources in the most luminous, on average more remote, galaxies which house the heftiest BHs.

The form of the ridge-line of the upper envelope, which approximately follows  $L_{\text{rad}} / M_{\text{BH}}^{2.0-2.5}$ , itself can be explained as an indirect by-product of two known, more fundamental correlations. Although the physical cause is not well understood, it has long been known that the integrated radio emission of early-type galaxies increases with their total optical luminosity (e.g., Auriemma et al. 1977; Fabbiano, Gioia, & Trinchieri 1989; Sadler, Jenkins, & Kotanyi 1989; Calvani, Fasano, & Franceschini 1989; Ho 1999b). The total mass (Heckman 1983) or pressure (Whittle 1992b) of the bulge component has been suggested as a parameter that could affect the efficacy of generating radio emission. In previous studies, the relation can be

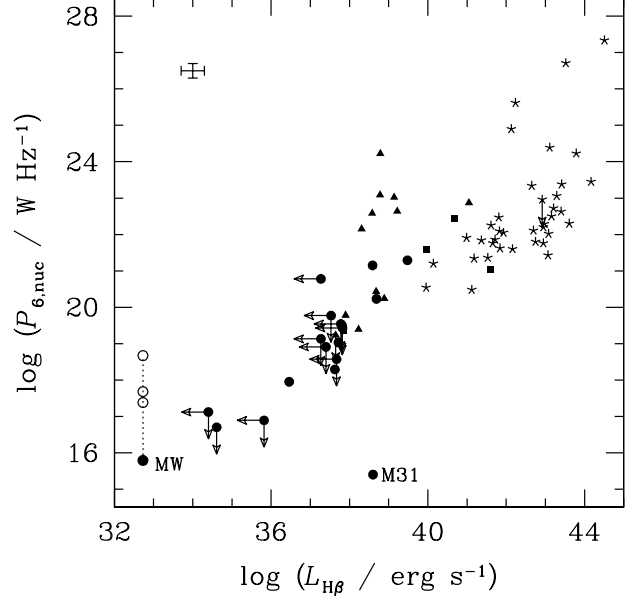


FIG. 4.— Correlation between nuclear 6 cm spectral power and  $H$  (broad + narrow components) luminosity. Symbols as in Figure 2. Representative error bars are plotted in the upper left corner; arrows indicate upper limits. We have labeled the outlier M31. Four values of  $P_{6,\text{nuc}}$  are given for the Milky Way (MW), connected by the dotted line; in increasing value, they are for Sgr A, Sgr A West, Sgr A West+East, and the central  $1' \times 1'$  ( $150 \text{ pc} \times 150 \text{ pc}$ ) (see § 2.3).

described as  $L_{\text{rad}} / L_{\text{opt}}$ , generally with  $L_{\text{rad}} / L_{\text{opt}} \sim 1-3$ . Figure 3 shows the strong correlation between total radio emission and integrated absolute  $B$  magnitude for our sample. The generalized Kendall's  $\tau$  test (Isobe, Feigelson, & Nelson 1986) returns a correlation coefficient of  $-1.1$  at a significance level  $> 99.99\%$ . A linear regression fit (solid line) using Schmitt's (1985) method gives  $\log P_{6,\text{tot}} / -0.99 M_{B_r}^0$ , or  $L_{\text{rad}} / L_{\text{opt}}^{2.5}$ . Now, since  $M_{\text{BH}}$  scales roughly linearly with the optical luminosity of the bulge (see references in § 1), which in bulge-dominated systems is comparable to the integrated light of the galaxy, it follows that  $L_{\text{rad}} / M_{\text{BH}}^{2.5}$ , as observed (Fig. 2a; solid line).

The active galaxies in Figure 2a do form a fairly well defined correlation, but this is simply a manifestation of the fact that for these objects the AGN component dominates the integrated emission, and, as we now argue, the relation between the nuclear radio power and  $M_{\text{BH}}$  is physically meaningful.

The distribution of  $P_{6,\text{nuc}}$  vs.  $M_{\text{BH}}$  also resembles an upper envelope (Fig. 2b), whose overall appearance is similar to that of the  $P_{6,\text{tot}}$  vs.  $M_{\text{BH}}$  diagram. Again, the weakly active galaxies do not trace the Franceschini et al. relation. The location of the points for Sgr A and the nucleus of M31 are particularly striking. They are the only objects with stellar-kinematical masses in the range  $M_{\text{BH}} \sim 10^6$  to few  $10^7 M$  that have detected radio cores. Both are extremely weak, with  $P_{6,\text{nuc}} < 10^{16} \text{ W Hz}^{-1}$ , approximately 3 orders of magnitude lower than the upper limits for the more distant galaxies. The position of the Galactic Center point, however, would migrate upwards (see points joined by dotted line) depending on one's definition of the "center," in which case M31 would be a distinct outlier. In any case, we suspect that the undetected galaxies could have tiny radio cores like Sgr A or the nucleus of M31 if they were to be observed at much higher sensitivity and resolution. Although the distribution of points in the lower right corner of

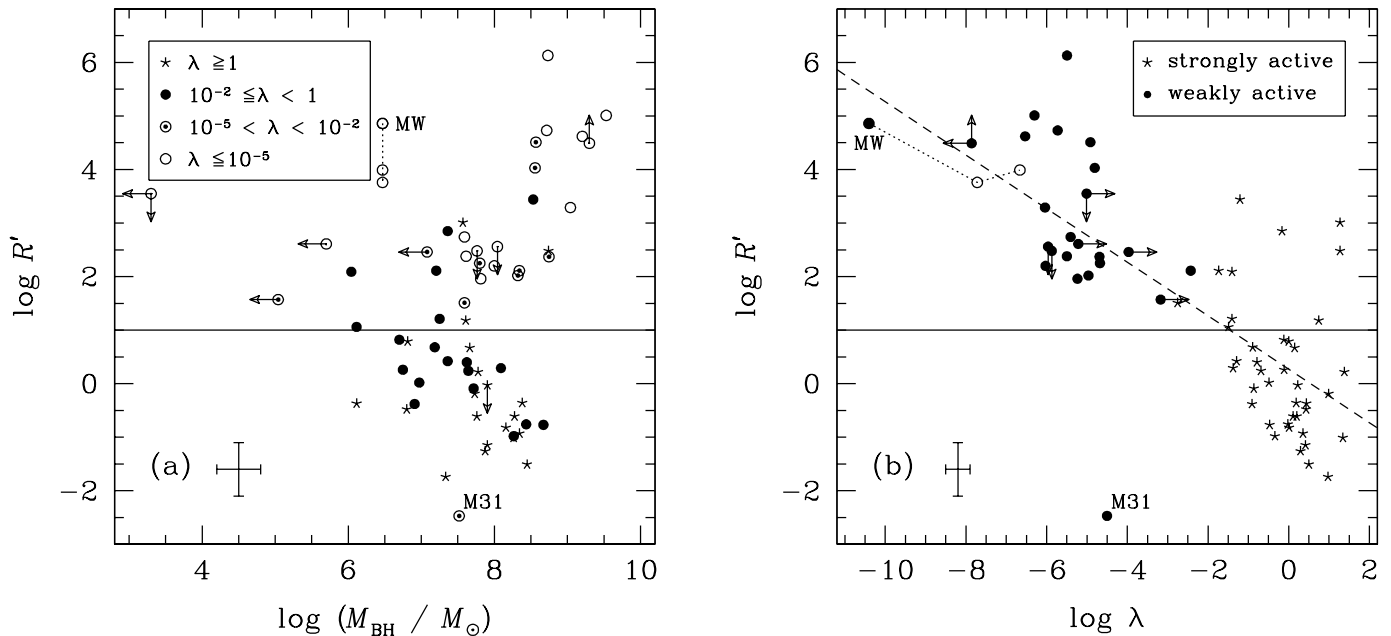


FIG. 5.— Distribution of the nuclear radio-to-optical luminosity ratio  $R^0$  (see text) versus (a) black hole mass and (b)  $L_{\text{bol}}=L_E$ . The solid line marks the formal division between radio-loud and radio-quiet objects,  $R^0 = 10$ . The dashed line in panel (b) is the best-fitting linear regression line. The legends indicate the meaning of the symbols. Representative error bars are plotted in the lower left corner of each panel; arrows indicate limits. The most massive BHs tend to be exceptionally radio-loud, highly sub-Eddington systems. We have labeled the outlier M31. Three points are plotted for the Milky Way (MW), connected by the dotted line; in increasing value of  $R^0$ , they are for Sgr A West, the central 1'' (150 pc 150 pc), and Sgr A (see § 2.3).

Figure 2b remains to be determined, it is likely that  $M_{\text{BH}}$  will continue to be a very poor predictor of radio power. Consider M31 and M81. Their BH masses differ by only a factor of 2, but the contrast in their radio core powers is a factor of nearly  $10^5$ .

The ridge-line of the upper envelope, on the other hand, is fairly well defined, and as in Figure 2a, the “zone of avoidance” in the upper left corner is genuine. Ignoring for the moment the handful of high-power sources with  $P_{6\text{puc}} > 10^{24} \text{ W Hz}^{-1}$ , it appears that at a given mass, the maximum core radio power increases roughly linearly with  $M_{\text{BH}}$ . A natural explanation for the functional form of the ridge-line can be found by appealing to Eddington-limited accretion and recognizing that radio power also scales roughly linearly with accretion (optical) luminosity for relatively active AGNs (Ho & Peng 2001), or equivalently, with mass accretion rate. It is worth remarking that the sample of the present study, although significantly more heterogeneous and diverse than that investigated by Ho & Peng (2001), also displays a reasonably strong correlation between radio and optical luminosity (Fig. 4)<sup>3</sup>. The maximum luminosity output of an accreting object in an isotropic, homogeneous system is set by the Eddington luminosity,  $L_E = 1.3 \times 10^{38} (M_{\text{BH}}/M_\odot) \text{ erg s}^{-1}$ . Setting  $L_{\text{bol}} = L_E$ , and approximating the bolometric luminosity with  $L_{\text{bol}} = c_B L_B = c_{B,r} P_{6\text{puc}}$ , we immediately arrive at  $P_{6\text{puc}} / M_{\text{BH}}^{1.4} = c_B / 1.3 \times 10^{38}$ . The constant  $c_B$  ranges from 11–17 for luminous AGNs and quasars (Sanders et al. 1989; Elvis et al. 1994) to 24 for very low-luminosity, possibly advection-dominated systems (median value for the 12 objects studied by Ho 1999c and Ho et al. 2000). The constant  $c_r$  can be obtained from the radio-optical continuum correlation of Ho & Peng (2001), and it differs slightly for radio-loud

compared to radio-quiet objects. The solid line in Figure 2b was obtained by choosing  $c_B = 17$  (Sanders et al. 1989) and the radio-loud branch of the  $P_{6\text{puc}} - M_B$  relation (Ho & Peng 2001). The agreement between the line and the boundary of the upper envelope is surprisingly good, both for the slope and the intercept. Nearly all of the AGNs fall in a band bracketed by  $L_{\text{bol}}/L_E = 0.01 - 1$ . Notably, many of the moderately active but lower luminosity AGNs (nearby Seyfert 2 nuclei and LINERs) whose masses have been determined by maser or ionized-gas kinematics are also broadly distributed among the more luminous AGNs. By contrast, the optically and radio quiescent systems, which comprise all the objects with stellar-based masses, uniformly occupy the highly sub-Eddington regime of the diagram. A small cluster of radio-luminous objects (e.g., 3C 120, 3C 273, 3C 351, 3C 390.3) lie above the  $L_{\text{bol}} = L_E$  line, but this is not unexpected because objects with powerful radio jets are known to follow a steeper radio-optical correlation (e.g., Serjeant et al. 1998; Willott et al. 1999).

### 3.2. Radio Loudness and Black Hole Mass

BH accretion in galactic nuclei invariably generates radio emission. The fundamental parameters responsible for the tremendous range of the observed strength of the radio output, however, are not well established and have been largely a subject of speculation. Recent advances in high-resolution imaging of quasars consistently suggest that radio-loud objects reside in hosts which lie on the top end of the galaxy luminosity function, whereas the hosts of radio-quiet sources generally span a wider range of luminosities. The degree of radio loudness, therefore, seems to depend on galaxy mass. In view of the link between BH mass and bulge mass (see § 1), it is reasonable to deduce

<sup>3</sup> As with the results reported in Ho & Peng (2001), we have confirmed that this correlation is not a spurious distance effect. See Ho & Peng for a discussion of the statistical method used to evaluate partial correlations with a third variable.

that radio loudness would depend on  $M_{\text{BH}}$ . Laor (2000) examined this issue using a sample of low-redshift ( $z < 0.5$ ) quasars from the Palomar-Green (PG) survey (Schmidt & Green 1983). The radio properties of the PG sources are known (Kellermann et al. 1989), and approximate virial masses can be estimated from the H  $\gamma$  line widths and optical continuum luminosities following empirical calibrations derived from AGN variability studies (Laor 1998; Kaspi et al. 2000). Laor (2000) concluded that the radio-loudness parameter  $R$  is a strong function of  $M_{\text{BH}}$ : most radio-loud objects (defined by  $\log R > 1$ ) have  $M_{\text{BH}} > 10^9 M_\odot$ , whereas nearly all quasars with  $M_{\text{BH}} < 3 \times 10^8 M_\odot$  are radio quiet.

The sample considered in this study, which spans a much wider gamut of activity level, yields a more complex picture. As shown in Figure 5a, the clean segregation in mass between radio-loud and radio-quiet objects suggested by Laor disappears. The radio-loud plane ( $\log R^0 > 1$ ) is richly populated with masses ranging from  $\log M_{\text{BH}} = 9.5$  to 6.0, and possibly even lower if we consider the upper limits. Indeed, most or all objects with  $\log M_{\text{BH}} > 8.5$  are radio loud, but radio-loud objects are by no means restricted to the high-mass domain.

To explore other factors which may govern the distribution of points on this plot, we have coded the symbols according to the bolometric luminosity of the nucleus normalized to the Eddington luminosity,  $L_{\text{bol}}/L_E$ . As in § 3.1, we estimate  $L_{\text{bol}}$  crudely from  $L_B$  (which is based on  $L_H$ ). An intriguing pattern emerges. The majority of sources with  $L_{\text{bol}} > 1$  land in the radio-quiet regime; those with  $L_{\text{bol}} < 10^{-5}$  fall exclusively in radio-loud territory; and objects with intermediate values of  $L_{\text{bol}}$  straddle the (somewhat arbitrary)  $R^0$  boundary. (M31 is a persistent outlier.) The dependence of  $R^0$  on  $L_{\text{bol}}$  is shown explicitly in Figure 5b; the objects form a striking inverse correlation, albeit with substantial scatter. The majority of the strongly active nuclei (Seyfert 1s and quasars) are characterized by  $\log L_{\text{bol}} > -2$  and  $\log R^0 < 1$ . With the exception of the deviant point for M31, all of the weakly active objects (those with  $M_{\text{BH}}$  based on spatially resolved kinematics) are confined to  $\log L_{\text{bol}} < -2$  and  $\log R^0 > 1$ . More quantitatively, the generalized Kendall's test, with M31 omitted, gives a correlation coefficient of  $-0.97$  at a significance level  $> 99.99\%$ . A linear regression fit (*dashed line*) using Schmitt's (1985) method, which treats censoring in both variables, gives

$$\log R^0 = -(0.50 \pm 0.07) \log L_{\text{bol}} + (0.27 \pm 0.24);$$

Since  $R^0$  depends on the mass accretion rate  $\dot{M}$  (see, e.g., Fig. 7 of Narayan et al. 1998b), an immediate consequence of the  $R^0$ – $L_{\text{bol}}$  inverse correlation is that the degree of radio loudness depends strongly on  $\dot{M}$ .

Although the strong inverse correlation between  $R^0$  and  $L_{\text{bol}}$  may superficially resemble a mutual dependence of these variables with optical luminosity ( $R^0 / L_B^{-1}$ ,  $L_{\text{bol}} / L_B$ ), we note that the slope of the  $R^0$ – $L_{\text{bol}}$  relation differs significantly from  $-1$ . We do not believe that this is the primary driver of the observed correlation.

#### 4. DISCUSSION AND SUMMARY

A number of statistical studies of luminous AGNs indicate that the processes responsible for the generation of radio sources depend directly on BH mass (McLure et al. 1999; Nelson 2000; Laor 2000; McLure & Dunlop 2001). Lacy et al. (2001) suggest that, in addition to the primary dependence on  $M_{\text{BH}}$ , the radio luminosity is also a weak function of  $L_{\text{bol}}$ .

Along similar lines, Franceschini et al. (1998) proposed that the weakly active nuclei in nearby galaxies also obey a correlation between radio luminosity and  $M_{\text{BH}}$ , roughly of the form  $L_{\text{rad}} / M_{\text{BH}}^{2.5}$ . The correlation evidently holds for the core radio emission as well as for the integrated radio emission. Franceschini et al. (1998) and Di Matteo et al. (2001) argue that the slope of the  $L_{\text{rad}}$ – $M_{\text{BH}}$  relation can be explained qualitatively in the context of advection-dominated accretion of hot plasma undergoing Bondi-type inflow. This interpretation, however, has been questioned by Yi & Boughn (1999), who noted that, given the observed radio powers and the critical assumption of Bondi accretion, the ADAF model predicts far more X-ray radiation than is actually detected.

We have reexamined these issues using a comprehensive compilation of up-to-date BH masses and photometric parameters. Our sample includes all the nearby, weakly active or inactive galaxies which have reliable BH masses determined through spatially resolved kinematics, as well as all the AGNs (Seyfert 1 nuclei and quasars) for which virial masses have been derived through reverberation mapping. Our main results lead to the following conclusions.

1. There is no simple relation between integrated radio luminosity and  $M_{\text{BH}}$ . The distribution of objects is consistent with either an upper envelope or a loose correlation of the form  $L_{\text{rad}} / M_{\text{BH}}^{2.0-2.5}$ , similar to that found by Franceschini et al. (1998), but we offer a different interpretation. We suggest that the integrated  $L_{\text{rad}}$ – $M_{\text{BH}}$  relation arises indirectly from two known, physically more fundamental correlations, namely that between integrated radio luminosity and optical bulge luminosity (mass) and that between bulge luminosity (mass) and BH mass.

2. There is no simple relation between core radio luminosity and  $M_{\text{BH}}$ . The distribution of objects appears to follow an upper envelope defined by Eddington-limited accretion. At any given value of  $M_{\text{BH}}$ , the maximum luminosity attained is set by  $L_{\text{bol}} = L_E$ , and as discussed by Ho & Peng (2001), the core radio power traces the accretion luminosity. The majority of the more active nuclei in our sample appear to be characterized by  $L_{\text{bol}} = (0.01 - 1)L_E$ . Not surprisingly, the more quiescent objects are radiating at only a tiny fraction of the Eddington rate.

3. There is no simple relation between the radio-loudness parameter  $R$  and  $M_{\text{BH}}$ . Specifically, we do not find the clean division between  $R$  and  $M_{\text{BH}}$  suggested by Laor (2000). Radio-loud nuclei are not confined solely to galaxies with the most massive BHs, but instead can inhabit galaxies with  $M_{\text{BH}}$  as low as  $10^6 M_\odot$ , or perhaps even less. The nucleus of the Milky Way provides an interesting, if unfamiliar, illustration. As a corollary of this result, radio-loud nuclei are not restricted to early-type (S0 and elliptical) galaxies, as conventionally thought; rather, they can be hosted by galaxies of a variety of morphological types, including disk-dominated spirals. Both of these results have been foreshadowed by recent investigations of the nuclear spectral energy distributions of nearby low-luminosity AGNs (Ho 1999c; Ho et al. 2000). Ho & Peng (2001) specifically challenged the traditional notion that Seyfert nuclei, the majority of which are hosted by disk galaxies, are primarily radio-quiet objects. Using high-resolution optical and radio measurements of a well-defined set of Seyfert 1 galaxies, they showed that the nuclear  $R$  parameter places more than 60% of the objects in the category of radio-loud sources ( $\log R > 1$ ). The present study proceeds in a similar spirit. In order to assess the relative radio power, we constructed nuclear measurements

of  $R^0$ , which differs from  $R$  only in that the optical continuum luminosity was obtained indirectly through the H luminosity. When studying nearby galaxies with low-luminosity nuclei, we reiterate the importance of using high-resolution data to properly define the *nuclear R* parameter — this is the quantity that is relevant for comparison with luminous AGNs and quasars, whose nonstellar nuclei dominate the integrated emission. We disagree with Laor’s (2000) use of single-dish radio measurements to evaluate the radio loudness of the objects in the sample of Ho (1999c). Laor also questioned the utility of the standard  $R$  parameter as applied to low-luminosity AGNs because he suspected that the optical bolometric correction may be exceptionally large for these objects. The characteristic weakness of the “big blue bump” in the spectral energy distributions of low-luminosity AGNs (Ho 1999c, 2001; Ho et al. 2000) indeed does lead to a larger value of  $L_{\text{bol}}=L_B$  than is typically seen in higher luminosity sources, but this difference is only a factor of 2 (see § 3.1), which is insufficient to alter the main conclusions.

4. We find a striking inverse correlation between  $R^0$  and  $L_{\text{bol}}=L_E$ . Since  $\dot{M}$  varies as a function of the mass accretion rate  $\dot{M}$ , the most straightforward implication of this result is that the relative radio power increases with decreasing  $\dot{M}$ . A significant fraction of the strongly active sources have high accretion rates ( $\log \dot{M} > -2$ ) and are radio quiet ( $\log R^0 < 1$ ), whereas nearly all of the weakly active objects are starved for fuel (all  $\log \dot{M} < -2$ ) and are radio loud ( $\log R^0 > 1$ ).

5. The systematic dependence of  $R$  on  $\dot{M}$  and the tendency for local galaxies to have nuclei which are both underluminous and radio loud are qualitatively consistent with predictions from accretion-disk theory. The amount of fuel available in the centers of present-day galaxies is plausibly quite low. As the accretion rate falls below a critical threshold of  $\dot{M} \approx 0.1 \text{ } ^2M_E \approx 0.01M_E$ , where  $\alpha$  is the standard viscosity parameter (assumed to have a value 0.3), the accretion flow makes a transition to an optically thin, two-temperature ADAF (Narayan et al. 1998b). Under these conditions, the low density and low optical depth of the accreting material lead to inefficient cooling, the radiative efficiency is much less than the canonical value of 10%, and thus the resulting luminosity

is low. Moreover, ADAFs produce generically “radio-loud” spectral energy distributions, for two reasons. First, cyclo-synchrotron emission at radio wavelengths provides energetically important cooling. And second, the broad-band spectrum, by definition, lacks the big blue bump usually attributed to thermal emission from the optically thick, geometrically thin disk (Shields 1978; Malkan & Sargent 1982). ADAFs are naturally bright in the radio and dim at optical/ultraviolet wavelengths: both conspire to boost  $R$ . The optical/ultraviolet component from an ADAF comes from inverse Compton scattering of the cyclo-synchrotron photons, and its strength increases sensitively with rising  $\dot{M}=\dot{M}_{\text{Edd}}$  (see e.g., Fig. 1 of Mahadevan 1997). This qualitatively explains the inverse correlation between  $R$  and  $\dot{M}$ . Furthermore, Rees et al. (1982) have suggested that the vertically thick structure of the “ion torus” may help facilitate the collimation of radio jets. Finally, we note that the majority of the weakly active objects in our sample have values of  $\dot{M} < 10^{-4} - 10^{-3}$ , comfortably below the threshold within which ADAFs operate. Although the above general arguments need to be confirmed with more quantitative calculations, a number of authors have invoked ADAF models to fit the spectral energy distributions of some of the objects in our sample (Sgr A, Manmoto, Mineshige, & Kusunose 1997, Narayan et al. 1998a; NGC 4258, Lasota et al. 1996, Chary et al. 2000; M81, Quataert et al. 1999; M87 and NGC 4649, Di Matteo et al. 2000).

I thank Marianne Vestergaard for discussions which motivated me to examine the issues discussed in this paper. Gary Bower kindly communicated information on M81 and NGC 3998 in advance of publication, and Swara Ravindranath helped to obtain *HST* photometry for a few objects. My research is supported in part by NASA grants HST-GO-06837.04-A, HST-AR-07527.03-A, and HST-AR-08361.02-A, awarded by the Space Telescope Science Institute, which is operated by AURA, Inc., under NASA contract NAS5-26555. This work made use of the NASA/IPAC Extragalactic Database (NED) which is operated by the Jet Propulsion Laboratory, California Institute of Technology, under contract with NASA, and of the Lyon-Meudon Extragalactic Database (LEDa).

## REFERENCES

- Antonucci, R. R. J. 1993, ARA&A, 31, 473  
Auremma, C., Perola, G. C., Ekers, R. D., Fanti, R., Lari, C., Jaffe, W. J., & Ulrich, M. H. 1977, A&A, 57, 41  
Baganoff, F. K., et al. 2001, ApJ, in press  
Barth, A. J., Sarzi, M., Rix, H.-W., Ho, L. C., Filippenko, A. V., & Sargent, W. L. W. 2001, ApJ, 555, 685  
Barvainis, R., Lonsdale, C., & Antonucci, R. 1996, AJ, 111, 1431  
Becker, R. H., White, R. L., & Edwards, A. L. 1991, ApJS, 75, 1  
Berkhuijsen, E. M. 1984, A&A, 140, 431  
Biretta, J., Stern, C. P., & Harris, D. E. 1991, AJ, 101, 1632  
Birkinshaw, M., & Davies, R. L. 1985, ApJ, 291, 32  
Blandford, R. D., & McKee, C. F. 1982, ApJ, 255, 419  
Böker, T., van der Marel, R., & Vacca, W. D. 1999, AJ, 118, 831  
Boroson, T. A., & Green, R. F. 1992, ApJS, 80, 109  
Bower, G. A., et al. 1998, ApJ, 492, L111  
———. 2001a, ApJ, 550, 75  
———. 2001b, in preparation  
Calvani, M., Fasano, G., & Franceschini, A. 1989, AJ, 97, 1319  
Cardelli, J. A., Clayton, G. C., & Mathis, J. S. 1989, ApJ, 345, 245  
Chary, R., Becklin, E. E., Evans, A. S., Neugebauer, G., Scoville, N. Z., Matthews, K., & Ressler, M. E. 2000, ApJ, 531, 756  
Condon, J. J. 1987, ApJS, 65, 485  
Condon, J. J., Cotton, W. D., Greisen, E. W., Yin, Q. F., Perley, R. A., Taylor, G. B., & Broderick, J. J. 1998, AJ, 115, 1693  
Crane, P. C., Dickel, J. R., & Cowan, J. J. 1992, ApJ, 390, L9  
Cretton, N., & van den Bosch, F. C. 1999, ApJ, 514, 704  
de Jong, R. S. 1996, A&A, 313, 377  
de Vaucouleurs, G., de Vaucouleurs, A., Corwin, H. G., Jr., Buta, R. J., Paturel, G., & Fouqué, R. 1991, Third Reference Catalogue of Bright Galaxies (New York: Springer) (RC3)  
Di Matteo, T., Carilli, C. L., & Fabian, A. C. 2001, ApJ, 547, 731  
Di Matteo, T., Quataert, E., Allen, S. W., Narayan, R., & Fabian, A. C. 2000, MNRAS, 311, 507  
Eckart, A., & Genzel, R. 1997, MNRAS, 284, 576  
Ekers, R. D., van Gorkom, J. H., Schwarz, U. J., & Goss, W. M. 1983, A&A, 122, 143  
Elmouttie, M., Haynes, R. F., Jones, K., Sadler, E. M., & Ehle, M. 1998, MNRAS, 297, 1202  
Elmouttie, M., Jones, K. L., Ehle, M., Beck, R., Harnett, J. I., & Wielebinski, R. 1997, MNRAS, 284, 830  
Elvis, M., et al. 1994, ApJS, 95, 1  
Emsellem, E., Dejonghe, H., & Bacon, R. 1999, MNRAS, 303, 495  
Fabbiano, G., Gioia, I. M., & Trinchieri, G. 1989, ApJ, 347, 127  
Faber, S. M., et al. 1997, AJ, 114, 1771  
Ferrarese, L., et al. 2000, ApJ, 529, 745  
Ferrarese, L., & Ford, H. C. 1999, ApJ, 515, 583  
Ferrarese, L., Ford, H. C., & Jaffe, W. 1996, ApJ, 470, 444  
Ferrarese, L., & Merritt, D. 2000, ApJ, 539, L9  
Ferrarese, L., Pogge, R. W., Peterson, B. M., Merritt, D., Wandel, A., & Joseph, C. L. 2001, ApJ, 555, L79  
Filippenko, A. V., & Ho, L. C. 2001, ApJ, submitted  
Franceschini, A., Vercellone, S., & Fabian, A. C. 1998, MNRAS, 297, 817

- Freeman, K. C., Karlsson, B., LyngA&A, G., Burrell, J. F., van Woerden, H., Goss, W. M., & Mebold, U. 1977, *A&A*, 55, 445
- Gaskell, C. M., & Ferland, G. J. 1984, *PASP*, 96, 393
- Gebhardt, K., et al. 2000a, *AJ*, 119, 1157
- . 2000b, *ApJ*, 539, L13
- . 2000c, *ApJ*, 543, L5
- . 2001, *AJ*, in press
- Genzel, R., Pichon, C., Eckart, A., Gerhard, O. E., & Ott, T. 2000, *MNRAS*, 317, 348
- Ghez, A. M., Klein, B. L., Morris, M., & Becklin, E. E. 1998, *ApJ*, 509, 678
- Greenhill, L. J., et al. 2000, in *IAU Symp. 205, Galaxies and their Constituents at the Highest Angular Resolutions*, ed. R. Schilizzi et al. (San Francisco: ASP), 54
- Greenhill, L. J., Gwinn, C. R., Antonucci, R., & Barvainis, R. 1996, *ApJ*, 472, L21
- Greenhill, L. J., Moran, J. M., & Herrnstein, J. R. 1997, *ApJ*, 481, L23
- Gregory, P. C., Vavasour, J. D., Scott, W. K., & Condon, J. J. 1994, *ApJS*, 90, 173
- Griffith, M. R., Wright, A. E., Burke, B. F., & Ekers, R. D. 1994, *ApJS*, 90, 179
- Gu, M., Cao, X., & Jiang, D. R. 2001, *MNRAS*, in press
- Halpern, J. P., Eracleous, M., Filippenko, A. V., & Chen, K. 1996, *ApJ*, 464, 704
- Hamilton, T. S., Casertano, S., & Turnshek, D. A. 2001, *ApJ*, in press
- Heckman, T. M. 1983, *ApJ*, 273, 505
- . 1996, in *The Physics of LINERs in View of Recent Observations*, ed. M. Eracleous et al. (San Francisco: ASP), 241
- Heckman, T. M., Balick, B., & Crane, P. C. 1980, *A&AS*, 40, 295
- Ho, L. C. 1999a, in *Observational Evidence for Black Holes in the Universe*, ed. S. K. Chakrabarti (Dordrecht: Kluwer), 157
- . 1999b, *ApJ*, 510, 631
- . 1999c, *ApJ*, 516, 672
- . 2001, in *Issues in Unification of AGNs*, ed. R. Maiolino, A. Marconi, & N. Nagar (San Francisco: ASP), in press
- Ho, L. C., et al. 2001, *ApJ*, 549, L51
- Ho, L. C., Filippenko, A. V., & Sargent, W. L. W. 1995, *ApJS*, 98, 477
- . 1996, *ApJ*, 462, 183
- . 1997, *ApJS*, 112, 315
- Ho, L. C., & Peng, C. Y. 2001, *ApJ*, 555, 650
- Ho, L. C., Rudnick, G., Rix, H.-W., Shields, J. C., McIntosh, D. H., Filippenko, A. V., Sargent, W. L. W., & Eracleous, M. 2000, *ApJ*, 541, 120
- Ho, L. C., & Ulvestad, J. S. 2001, *ApJS*, 133, 77
- Hummel, E., van der Hulst, J. M., & Dickey, J. M. 1984, *A&A*, 134, 207
- Hummel, E., van der Hulst, J. M., Keel, W. C., & Kennicutt, R. C., Jr. 1987, *A&AS*, 70, 517
- Isobe, T., Feigelson, E. D., & Nelson, P. I. 1986, *ApJ*, 306, 490
- Jenkins, C. R., Pooley, G. C., & Riley, J. M. 1977, *MNRAS*, 84, 61
- Jones, D. H., et al. 1996, *ApJ*, 466, 742
- Jones, D. L., et al. 1986, *ApJ*, 305, 684
- Kaspi, S., Smith, P. S., Netzer, H., Maoz, D., Jannuzi, B. T., & Givon, U. 2000, *ApJ*, 533, 631
- Kellermann, K. I., Sramek, R. A., Schmidt, M., Green, R. F., Shaffer, D. B. 1994, *AJ*, 108, 1163
- Kellermann, K. I., Sramek, R. A., Schmidt, M., Shaffer, D. B., & Green, R. F. 1989, *AJ*, 98, 1195
- Kormendy, J. 1993, in *The Nearest Active Galaxies*, ed. J. Beckman, L. Colina, & H. Netzer (Madrid: Consejo Superior de Investigaciones Científicas), 197
- Kormendy, J., et al. 1997a, *ApJ*, 473, L91
- . 1997b, *ApJ*, 482, L139
- . 2001, *ApJ*, submitted
- Kormendy, J., & Bender, R. 1999, *ApJ*, 522, 772
- Kormendy, J., & Gebhardt, K. 2001, in *The 20th Texas Symposium on Relativistic Astrophysics*, ed. H. Martel & J. C. Wheeler (New York: AIP), in press
- Kormendy, J., & Richstone, D. O. 1995, *ARA&A*, 33, 581
- Koyama, K., Maeda, Y., Sonobe, T., Takeshima, T., Tanaka, Y., & Yamauchi, S. 1996, *PASJ*, 48, 249
- Krolik, J. H. 2001, *ApJ*, 551, 72
- Kukula, M. J., Pedlar, A., Baum, S. A., O'Dea, C. P. 1995, *MNRAS*, 276, 1262
- Lacy, M., Laurent-Meuleisen, S. A., Ridgway, S. E., Becker, R. H., & White, R. L. 2001, *ApJ*, 551, L17
- Laor, A. 1998, *ApJ*, 505, L83
- . 2000, *ApJ*, 543, L111
- Lasota, J.-P., Abramowicz, M. A., Chen, X., Krolik, J., Narayan, R., & Yi, I. 1996, *ApJ*, 462, 142
- Lauer, T. R., et al. 1995, *AJ*, 110, 2622
- Macchetto, F., Marconi, A., Axon, D. J., Capetti, A., Sparks, W. B., & Crane, P. 1997, *ApJ*, 489, 579
- Magorrian, J., et al. 1998, *AJ*, 115, 2285
- Mahadevan, R. 1997, *ApJ*, 477, 585
- Malhotra, S., Spigel, D. N., Rhoads, J. E., & Li, J. 1996, *ApJ*, 473, 687
- Malkan, M. A., & Sargent, W. L. W. 1982, *ApJ*, 254, 22
- Manmoto, T., Mineshige, S., & Kusunose, M. 1997, *ApJ*, 489, 791
- Maoz, E. 1998, *ApJ*, 494, L181
- McCall, M. L. 1989, *AJ*, 97, 1341
- McLure, R. J., & Dunlop, J. S. 2001, *MNRAS*, 327, 199
- McLure, R. J., Dunlop, J. S., Kukula, M. J., Baum, S. A., O'Dea, C. P., & Hughes, D. H. 1999, *MNRAS*, 308, 377
- Mezger, P. G., & Pauls, T. 1979, in *IAU Symp. 84*, ed. W. B. Burton (Dordrecht: Reidel), 357
- Miyoshi, M., Moran, J., Herrnstein, J., Greenhill, L., Nakai, N., Diamond, P., & Inoue, M. 1995, *Nature*, 373, 127
- Moorwood, A. F. M., & Oliva, E. 1988, *A&A*, 203, 278
- Morganti, R., Fanti, R., Fanti, C., Parma, P., & de Ruiter, H. 1987, *A&A*, 183, 203
- Morganti, R., Ulrich, M.-H., & Tadhunter, C. N. 1992, *MNRAS*, 254, 546
- Narayan, R., Mahadevan, R., Grindlay, J. E., Popham, R. G., & Gammie, C. 1998a, *ApJ*, 492, 554
- Narayan, R., Mahadevan, R., & Quataert, E. 1998b, in *The Theory of Black Hole Accretion Discs*, ed. M. A. Abramowicz, G. Björnsson, & J. E. Pringle (Cambridge: Cambridge Univ. Press), 148
- Nelson, C. H. 2000, *ApJ*, 544, L91
- Newman, J. A., Eracleous, M., Filippenko, A. V., & Halpern, J. P. 1997, *ApJ*, 485, 570
- Oke, J. B., & Goodrich, R. W. 1981, *ApJ*, 243, 445
- Oliva, E., Salvati, M., Moorwood, A. F. M., & Marconi, A. 1994, *A&A*, 288, 457
- Osterbrock, D. E. 1989, *Astrophysics of Gaseous Nebulae and Active Galactic Nuclei* (Mill Valley: Univ. Science Books)
- Puschell, J. J., Moore, R., Cohen, R. D., Owen, F. N., & Phillips, A. C. 1986, *AJ*, 91, 751
- Quataert, E. 2001, in *Probing the Physics of Active Galactic Nuclei by Multiwavelength Monitoring*, ed. B. M. Peterson, R. S. Polidan, & R. W. Pogge (San Francisco: ASP), 71
- Quataert, E., Di Matteo, T., Narayan, R., & Ho, L. C. 1999, *ApJ*, 525, L89
- Ravindranath, S., Ho, L. C., Peng, C. Y., Filippenko, A. V., & Sargent, W. L. W. 2001, *AJ*, 122, 653
- Reid, M. J. 1993, *ARA&A*, 31, 345
- Rees, M. J., Begelman, M. C., Blandford, R. D., & Phinney, E. S. 1982, *Nature*, 295, 17
- Richstone, D. O., et al. 1998, *Nature*, 395, A14
- Rush, B., Malkan, M. A., & Edelson, R. A. 1996, *ApJ*, 473, 130
- Sadler, E. M., Jenkins, C. R., & Kotanyi, C. G. 1989, *MNRAS*, 240, 591
- Salucci, P., Szuszkiewicz, E., Monaco, P., & Danese, L. 1999, *MNRAS*, 307, 637 (erratum: *MNRAS*, 311, 448)
- Sanders, D. B., Phinney, E. S., Neugebauer, G., Soifer, B. T., & Matthews, K. 1989, *ApJ*, 347, 29
- Sarzi, M., Rix, H.-W., Shields, J. C., Rudnick, G., Ho, L. C., McIntosh, D. H., Filippenko, A. V., & Sargent, W. L. W. 2001, *ApJ*, 550, 65
- Schlegel, D. J., Finkbeiner, D. P., & Davis, M. 1998, *ApJ*, 500, 525
- Schmidt, M., & Green, R. F. 1983, *ApJ*, 269, 352
- Schmitt, J. H. M. M. 1985, *ApJ*, 293, 178
- Serjeant, S., Rawlings, S., Maddox, S. J., Baker, J. C., Clements, D., Lacy, M., & Lilje, P. B. 1998, *MNRAS*, 294, 494
- Shields, G. A. 1978, *Nature*, 272, 706
- Shuder, J. M. 1981, *ApJ*, 244, 12
- Shuder, J. M., & Osterbrock, D. E. 1981, *ApJ*, 250, 55
- Singh, K. P., & Westergaard, N. J. 1992, *A&A*, 264, 489
- Spencer, R. E., & Junor, W. 1986, *Nature*, 321, 753
- Stoeck, J. T., Morris, S. L., Weymann, R. J., & Foltz, C. B. 1992, *ApJ*, 396, 487
- Tadhunter, C. N., Morganti, R., di Serego Alighieri, S., Fosbury, R. A. E., & Danziger, I. J. 1993, *MNRAS*, 263, 999
- Tonry, J., Dressler, A., Blakeslee, J. P., Ajhar, E. A., Fletcher, A. B., Luppino, G. A., Metzger, M. R., & Moore, C. B. 2001, *ApJ*, 546, 681
- Tully, R. B. 1988, *Nearby Galaxies Catalog* (Cambridge: Cambridge Univ. Press)
- Turner, J. L., & Ho, P. T. P. 1983, *ApJ*, 268, L79
- Ulvestad, J. S., & Wilson, A. S. 1984a, *ApJ*, 278, 544
- . 1984b, *ApJ*, 285, 439
- Unger, S. W., Lawrence, A., Wilson, A. S., Elvis, M., & Wright, A. E. 1987, *MNRAS*, 228, 521
- van den Bosch, F. C., & van der Marel, R. P. 1995, *MNRAS*, 274, 884
- van der Marel, R. P. 1999, in *IAU Symp. 186, Galaxy Interactions at Low and High Redshift*, ed. J. E. Barnes & D. B. Sanders (Dordrecht: Kluwer), 333
- van der Marel, R. P., Cretton, N., de Zeeuw, P. T., & Rix, H.-W. 1998, *ApJ*, 493, 613
- van der Marel, R. P., & van den Bosch, F. C. 1998, *AJ*, 116, 2220
- Verdoes Kleijn, G. A., van der Marel, R. P., Carollo, C. M., & de Zeeuw, P. T. 2000, *AJ*, 120, 1221
- Visnovsky, K. L., Impey, C. D., Foltz, C. B., Hewett, P. C., Weymann, R. J., & Morris, S. L. 1992, *ApJ*, 391, 560
- Wandel, A. 1999, *ApJ*, 519, L39
- Wandel, A., Peterson, B. M., & Malkan, M. A. 1999, *ApJ*, 526, 579
- White, R. L., & Becker, R. H. 1992, *ApJS*, 79, 331
- Whittle, M. 1992a, *ApJS*, 79, 49
- . 1992b, *ApJ*, 387, 121
- Willott, C. J., Rawlings, S., Blundell, K. M., & Lacy, M. 1999, *MNRAS*, 309, 1017
- Wright, A. E., Griffith, M. R., Hunt, A. J., Troup, E., Burke, B. F., & Ekers, R. D. 1996, *ApJS*, 103, 145
- Wrobel, J. M., & Heeschen, D. S. 1984, *ApJ*, 287, 41
- . 1991, *AJ*, 101, 148

Yee, H. K. C. 1980, ApJ, 241, 894

Yi, I., & Boughn, S. P. 1999, ApJ, 515, 576